

Satellite clear-sky observations overestimate surface urban heat islands in humid cities

Qiquan Yang^{1, 2, 3}, Yi Xu¹, Dawei Wen⁴, Ting Hu⁵, TC Chakraborty⁶, Yue Liu⁷, Rui Yao⁸,

Shurui Chen², Changjiang Xiao^{2, 3}, Jie Yang⁸

¹ State Key Laboratory of Lunar and Planetary Sciences, Macau University of Science and Technology, Macau, China

² College of Surveying & Geo-Informatics, Tongji University, Shanghai 200092, China

³ The Shanghai Key Laboratory of Space Mapping and Remote Sensing for Planetary Exploration, Tongji University, Shanghai 200092 China

⁴ School of Computer Science and Engineering, Hubei Key Laboratory of Intelligent Robot, Wuhan Institute of Technology, Wuhan 430205, China

⁵ School of Remote Sensing and Geomatics Engineering, Nanjing University of Information Science and Technology, Nanjing 210044, China

⁶ Pacific Northwest National Laboratory, Richland, WA, USA

⁷ Guangzhou Institute of Geography, Guangdong Academy of Sciences, Guangzhou 510070, China

⁸ School of Remote Sensing and Information Engineering, Wuhan University, Wuhan 430079, China

Corresponding author: Yi Xu (yixu@must.edu.mo)

Contents of this file

Text S1

Figures S1 to S3

Tables S1 to S3

Text S1: Some details about data and methods

The Global Urban Boundary (GUB) offers a high-resolution delineation of global urban areas from 1990 to 2018 with a five-year interval, and the data of 2015 was selected in this study. Firstly, The GUB patches located within a proximity of less than 2 km were consolidated into the same urban clusters. Then, 639 urban clusters were randomly selected across globe. All these urban clusters exceed 100 km² in size and serve as representations of the urban areas of each city. Choosing larger cities helps to highlight the differences in sky conditions between urban and rural areas since sky conditions at smaller scales tend to be spatially similar.

All-sky LST was derived from the Global Seamless and High-resolution Temperature Dataset (GSHTD). It was produced by fusing the MODIS and the ERA5-land reanalysis LST observations through a developed method called the estimation of the temperature difference. Validation results showed a good spatial agreement ($R^2 > 0.8$) between the reconstructed and in-situ LST observations. Consistent with the all-sky LST, the clear-sky LST was derived from the MODIS LST products (MOD11A2). The clear-sky LST dataset may potentially exhibit missing values due to the absence of measurements during cloudy conditions. The spatial coverage of both the all-sky and clear-sky LST datasets remains consistent, encompassing the entire globe. In our analysis, we conducted separate annual and seasonal averaging for these datasets. For cities in the Northern Hemisphere (Southern Hemisphere), spring is observed from March to May (September to November), summer from June to August (December to February), autumn from September to November (March to May), and winter from December to February (June to August).

The Modified Equal Area-Rural (MEA-R) method was used for determining background rural area when estimating SUHII. The basic idea of this method is as follows: (1) Construct buffers around the central urban area through an iterative process. In each iteration, water bodies and elevation anomalies within the buffer were removed until the remaining buffer area closely approximated twice the size of the urban area. (2) Calculate the median NLI within the resultant buffer and remove the portion of the buffer where the NLI exceeds this median value. The remaining parts of the buffer were then regarded as the rural area.

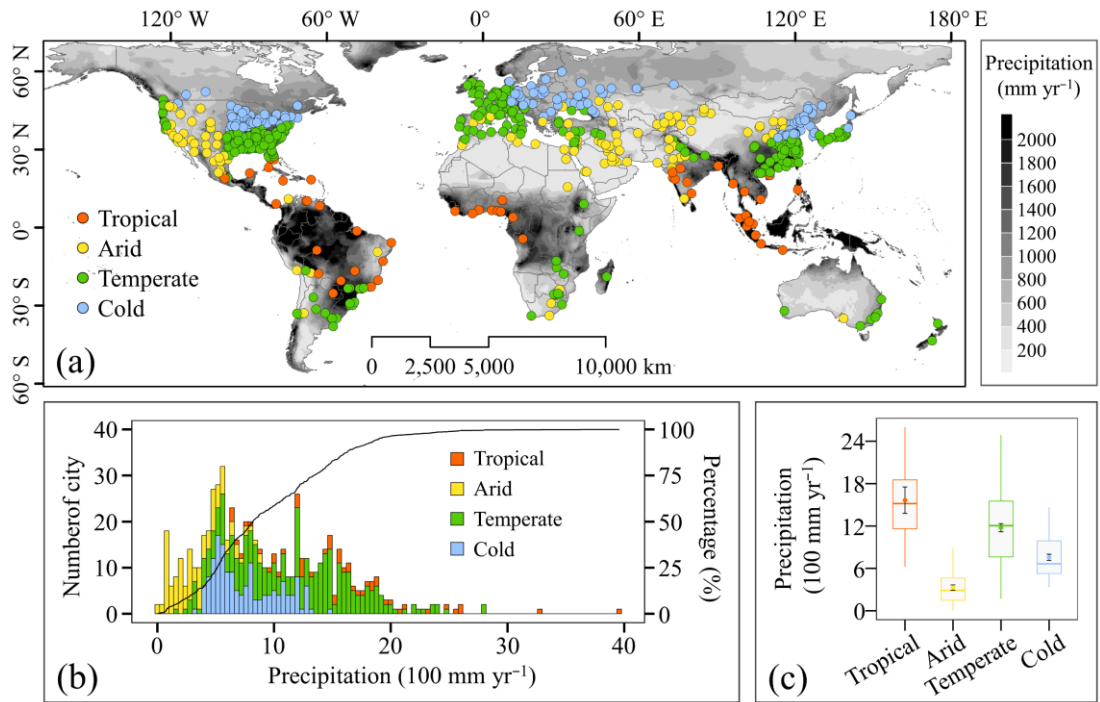


Figure S1. Spatial distribution and annual precipitation for global 639 cities. (a) Locations of cities. (b) Precipitation histogram for global cities. (c) Boxplots of precipitation for cities located in different climate zones. The colored points and black error bars in (c) represent the mean values and 95% confidence intervals, respectively.

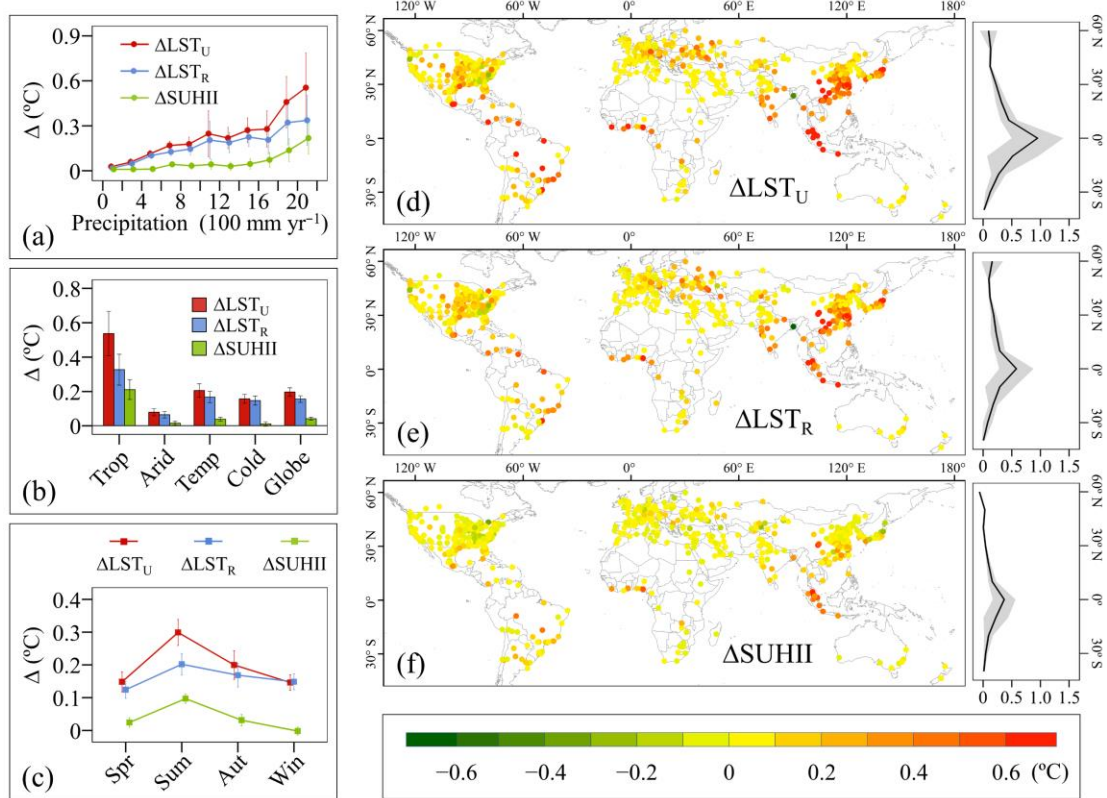


Figure S2. Clear-sky and all-sky differences in SUHII (Δ SUHII), urban average LST (Δ LST_U), and rural average LST (Δ LST_R). (a) Annual nighttime averages of different precipitation intervals. (b) Annual nighttime averages for different climate zones (tropical zone (Trop), arid zone (Arid), temperate zone (Temp), and cold zone (Cold)). (c) Nighttime averages for global cities across seasons (spring (Spr), summer (Sum), Autumn (Aut), and Winter (Win)). (d-f) Spatial distributions of annual nighttime Δ LST_U, Δ LST_R, and Δ SUHII. Error bars in (a-c) and shaded areas in (d-f) represent 95% confidence intervals.

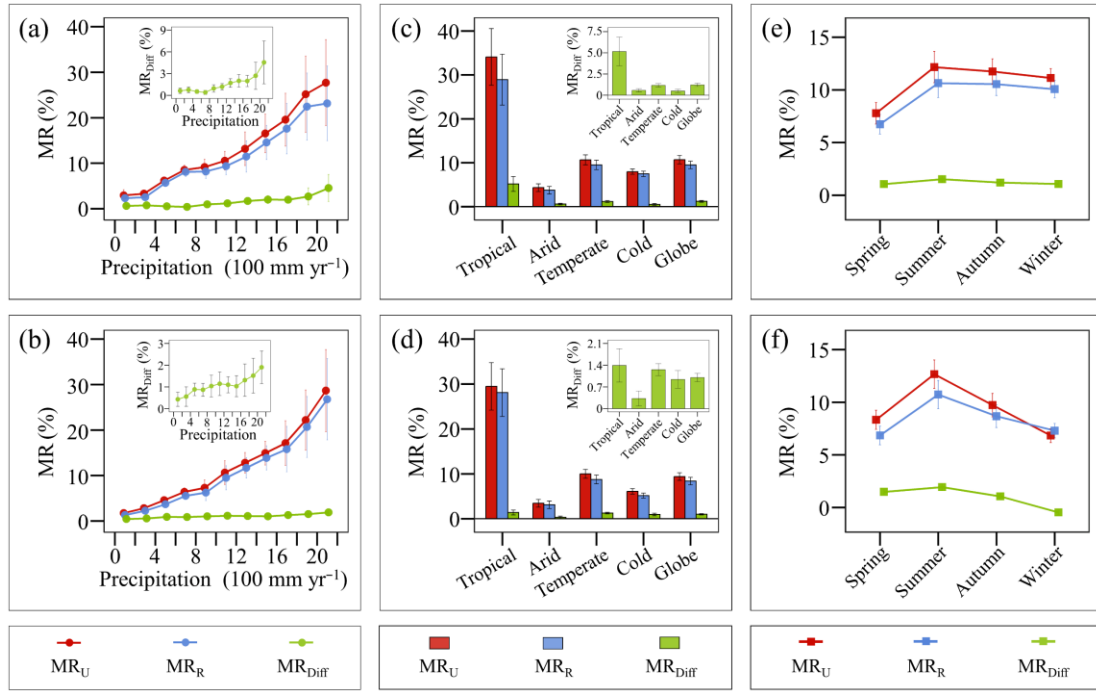


Figure S3. Missing rate (MR) of clear-sky LST observations. (a-b) Annual daytime and nighttime averages of different precipitation intervals. (c-d) Annual daytime and nighttime averages of different climate zones. (e-f) Seasonal daytime and nighttime averages for global cities. MR_U and MR_R refer to MR for the urban area and the rural area, respectively. The difference between MR_U and MR_R is represented as MR_{Diff}. Error bars in (a-f) represent 95% confidence intervals.

Table S1. Description of the datasets used in this study

Data	Usage	Resolution	Period	Access link
Global Urban Boundary (GUB) dataset	Capturing the boundaries of urban extents	30 m	2015	http://data.starcloud.pcl.ac.cn/zh/resource/14
Global Seamless and High-resolution Temperature Dataset (GSHTD)	Acquisition of all-sky LST observations	1 km	2014-2016	https://www.researchgate.net/publication/366556370_Global_seamless_and_high-resolution_temperature_dataset_GSHTD_2001-2020
MODIS LST product	Acquisition of clear-sky LST observations	1 km	2014-2016	https://e4ftl01.cr.usgs.gov/MOLT/MOD11A2.061/
VIIRS nighttime light product	Removal of the interference of human activities on SUHII estimations	500 m	2015	https://ladsweb.modaps.eosdis.nasa.gov/search/order/1/VIIRS:Suomi-NPP
Global 30 Arc-Second Elevation (GTOPO30) data	Minimizing the influence of topographic relief on SUHII estimations	1 km	/	https://www.usgs.gov/centers/eros/science/usgs-eros-archive-digital-elevation-global-30-arc-second-elevation-gtopo30
Global Surface Water (GSW) data	Eliminating the influence of water bodies on SUHII estimations	30 m	2015	https://global-surface-water.appspot.com/download
TerraClimate dataset	Acquisition of annual precipitation	4 km	2014-2016	https://www.climatologylab.org/terraclimate.html
Köppen–Geiger climate map	Delineation of the climatic zone to which the city belongs	1 km	/	http://www.gloh2o.org/koppen/

Table S2. Averages of clear-sky SUHI, all-sky SUHI, and their difference (Δ)

			Tropical (°C)	Arid (°C)	Temperate (°C)	Cold (°C)	Globe (°C)
Annual	Day	Clear-sky	2.97 ± 0.43	−0.39 ± 0.30	1.60 ± 0.13	1.19 ± 0.16	1.23 ± 0.12
		All-sky	2.32 ± 0.34	−0.42 ± 0.30	1.50 ± 0.13	1.15 ± 0.15	1.12 ± 0.11
		Δ	0.65 ± 0.18	0.03 ± 0.01	0.09 ± 0.02	0.04 ± 0.02	0.11 ± 0.02
	Night	Clear-sky	1.35 ± 0.17	1.55 ± 0.15	1.12 ± 0.06	1.48 ± 0.09	1.31 ± 0.05
		All-sky	1.13 ± 0.18	1.53 ± 0.15	1.08 ± 0.06	1.47 ± 0.09	1.27 ± 0.05
		Δ	0.21 ± 0.06	0.02 ± 0.01	0.04 ± 0.01	0.01 ± 0.01	0.04 ± 0.00
Summer	Day	Clear-sky	3.41 ± 0.45	−0.35 ± 0.46	2.58 ± 0.21	2.50 ± 0.23	2.08 ± 0.17
		All-sky	2.37 ± 0.37	−0.38 ± 0.45	2.41 ± 0.20	2.45 ± 0.23	1.89 ± 0.16
		Δ	1.04 ± 0.31	0.03 ± 0.02	0.17 ± 0.04	0.05 ± 0.02	0.19 ± 0.04
	Night	Clear-sky	1.09 ± 0.18	1.63 ± 0.18	1.41 ± 0.07	1.79 ± 0.11	1.52 ± 0.06
		All-sky	0.84 ± 0.18	1.61 ± 0.18	1.31 ± 0.07	1.70 ± 0.10	1.42 ± 0.06
		Δ	0.25 ± 0.08	0.02 ± 0.02	0.10 ± 0.02	0.09 ± 0.02	0.10 ± 0.01
Winter	Day	Clear-sky	2.50 ± 0.47	−0.25 ± 0.23	0.66 ± 0.09	0.47 ± 0.15	0.59 ± 0.09
		All-sky	2.23 ± 0.40	−0.31 ± 0.23	0.62 ± 0.09	0.40 ± 0.14	0.52 ± 0.09
		Δ	0.27 ± 0.15	0.06 ± 0.04	0.04 ± 0.02	0.07 ± 0.04	0.07 ± 0.02
	Night	Clear-sky	1.60 ± 0.24	1.46 ± 0.17	0.81 ± 0.08	1.27 ± 0.16	1.11 ± 0.07
		All-sky	1.51 ± 0.25	1.44 ± 0.17	0.83 ± 0.08	1.29 ± 0.15	1.11 ± 0.07
		Δ	0.09 ± 0.05	0.02 ± 0.02	−0.02 ± 0.02	−0.02 ± 0.03	0.00 ± 0.01

Mean ± 95% confidence interval.

Table S3. Diurnal and seasonal contrasts in clear-sky SUHI, all-sky SUHI and their difference (Δ)

		Tropical (°C)	Arid (°C)	Temperate (°C)	Cold (°C)	Globe (°C)
Diurnal difference (day – night)						
Annual	Clear-sky	1.62 ± 0.50	-1.94 ± 0.32	0.47 ± 0.16	-0.29 ± 0.19	-0.07 ± 0.14
	All-sky	1.18 ± 0.42	-1.96 ± 0.32	0.42 ± 0.15	-0.31 ± 0.18	-0.15 ± 0.13
	Δ	0.44 ± 0.16	0.02 ± 0.02	0.05 ± 0.02	0.02 ± 0.02	0.08 ± 0.02
Summer	Clear-sky	2.32 ± 0.47	-1.97 ± 0.46	1.17 ± 0.21	0.72 ± 0.25	0.56 ± 0.18
	All-sky	1.53 ± 0.35	-1.98 ± 0.46	1.10 ± 0.20	0.75 ± 0.24	0.47 ± 0.17
	Δ	0.79 ± 0.02	0.01 ± 0.02	0.07 ± 0.04	-0.03 ± 0.02	0.09 ± 0.03
Winter	Clear-sky	0.90 ± 0.59	-1.71 ± 0.30	-0.15 ± 0.14	-0.80 ± 0.22	-0.52 ± 0.13
	All-sky	0.72 ± 0.55	-1.75 ± 0.30	-0.21 ± 0.13	-0.89 ± 0.20	-0.59 ± 0.12
	Δ	0.18 ± 0.12	0.04 ± 0.04	0.06 ± 0.02	0.09 ± 0.05	0.07 ± 0.02
Seasonal difference (summer – winter)						
Day	Clear-sky	0.91 ± 0.36	-0.09 ± 0.39	1.93 ± 0.16	2.04 ± 0.22	1.49 ± 0.14
	All-sky	0.14 ± 0.42	-0.06 ± 0.38	1.79 ± 0.15	2.05 ± 0.21	1.37 ± 0.14
	Δ	0.77 ± 0.30	-0.03 ± 0.04	0.14 ± 0.04	-0.01 ± 0.05	0.12 ± 0.04
Night	Clear-sky	-0.51 ± 0.24	0.17 ± 0.18	0.60 ± 0.09	0.52 ± 0.18	0.41 ± 0.08
	All-sky	-0.67 ± 0.24	0.17 ± 0.18	0.48 ± 0.09	0.41 ± 0.17	0.31 ± 0.07
	Δ	0.16 ± 0.07	0.00 ± 0.03	0.12 ± 0.03	0.11 ± 0.04	0.10 ± 0.02

Mean ± 95% confidence interval.